Available online at www.sciencedirect.com
SCIENCE DIRECT®
Solid-State Electronics 48 (2004) 1795–1799
SOLID-STATE ELECTRONICS
www.elsevier.com/locate/sse

Effects of microwave interference on the operational parameters of n-channel enhancement mode MOSFET devices in CMOS integrated circuits

Kyechong Kim *, Agis A. Iliadis, Victor L. Granatstein

Electrical and Computer Engineering Department, University of Maryland, College Park, MD 20742, USA

Received 10 December 2003; accepted 15 March 2004
Available online 25 June 2004

Abstract

The effects of microwave interference on the operational parameters of individual MOSFET devices on CMOS wafers were studied as microwave power and frequency were varied. The study used direct injection of microwave power into the device terminals, and the output characteristics were measured with and without the microwave interference. The study showed that injected microwave power significantly affects output current, transconductance, output conductance, and breakdown voltage for power levels above 10 dBm in the frequency range between 1 and 20 GHz. The effects result in the devices loosing switching-off capability, saturation and linearity in the amplification region of their output characteristics, and developing DC offset currents at zero drain bias, while breakdown shifts to significantly lower voltages. Most importantly the sensitivity to microwave power was strongly suppressed at frequencies above 5 GHz indicating the possibility of a by-pass path for the injected power through intrinsic capacitive coupling of the devices to ground.

1. Introduction

Electromagnetic interference (EMI) can couple into electronic modules and systems intentionally from high power microwave (HPM) or ultra-wide band (UWB) sources or unintentionally due to the proximity to sources or general environmental RF signals, and cause significant "soft" reversible errors (bit flipping, delay/response, noise/distortion level, gain disruption, and others) and "hard" irreversible errors (gate oxide breakdown, junction filamentation, avalanche breakdown, metallization/interconnect peel-off, and others). It has been reported that portable HPM sources can cause serious upset in commercially available electronic systems from a maximum distance of 500 m, and hand-held HPM units located in suitcases can cause upsets from a distance of 50 m, and permanent damage at a distance of 15 m [1]. Protection in the form of shielding [2,3] and special design of operational amplifiers [4] have been considered for reducing this hazard but still for high power interference, connecting wires, microslits in sealed (packaged) chips, and the input/output leads of packaged chips, as well as actual antennas for mobile communication units, can become effective inputs to couple the EMI into the integrated circuit. Electrostatic discharge (ESD) protection on-chip may not be effective enough to protect or may even, in some cases, enhance the effects of the interference [5] from the induced radiation propagating through leads and microslits to the packaged chip enclosure. Currently, our understanding of these effects is limited and more systematic work is necessary to clarify the effects first at the device level, and then at the circuit and system levels. This work examines the effects on individual MOSFET devices which constitute the basic units in IC CMOS circuits, and focuses on micron and sub-micron n-channel

* Corresponding author.
E-mail address: kyechong@umd.edu (K. Kim).

0038-1101/$ - see front matter © 2004 Elsevier Ltd. All rights reserved.
doi:10.1016/j.sse.2004.05.015

enhancement mode MOSFET devices where the microwave interference is direct injected into the input/output leads of the device. The operational parameters and s-parameters are measured prior, during and after the interference event.

2. Experimental details

In order to be able to monitor the effects without frequent burn-out of the devices, gate lengths between 2 and 20 μm on (1 0 0) 3′ p-type Si wafers were examined first. The chips that contained individual devices with varying gate lengths, where packaged and placed on a specially designed PC board for measurements. A controlled RF signal was injected first into the gate, and then into the drain and the output characteristics were measured using a HP 4145 semiconductor device parameter analyzer. Input RF power and frequency were varied from 0 to 30 dBm and 1 to 20 GHz, respectively. Submicron (0.5 μm) gate n-channel enhancement mode MOSFETs were also examined in this work. These chips of individual MOSFETs were unpackaged and the devices were directly probed using the Cascade Microwave probe system and the HP 8510 network analyzer. Input RF power was varied from 0 to 20 dBm at a frequency between 1 and 20 GHz.

3. Experimental results and discussion

RF injection at the gate of the device had a profound effect on the output I–V characteristics for power levels above 10 dBm, and made the devices inoperable at 30 dBm as shown in Figs. 1 and 2. The device characteristics show a gradual increase in output drain current with injected power levels, a gradual loss of saturation,

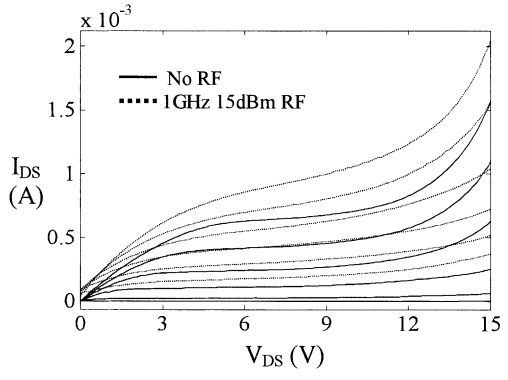

Fig. 1. Output current I_{DS} versus input bias V_{DS} with and without RF injection to the gate. Output current increase and positive offset current at zero drain bias are observed at power 15 dBm, 1 GHz.

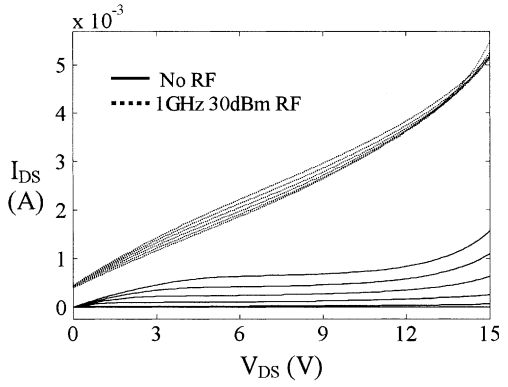

Fig. 2. Output current I_{DS} versus input bias V_{DS} with and without RF injection to the gate. Induced RF field, power 30 dBm, 1 GHz, drives the channel into deep inversion to an approximately uniform channel that reaches no pinch-off at the drain for saturation to occur.

and a positive offset current at zero drain bias, suggesting that the induced RF field at the gate drives the channel into deep inversion to an approximately uniform channel that reaches no pinch-off at the drain for saturation to occur.

The collapse of the characteristic allows no effective channel modulation by the gate, and the substantially increased current levels, render the device well outside the set operational limits for the circuit. In addition at higher frequencies (>5 GHz) the RF power effects were found to be strongly suppressed by the increased frequency, as shown in Fig. 3. A plot of the difference of drain current, ΔI_D, measured from the I–V characteristics with and without RF injection at the gate is shown in Fig. 4. The plot shows significant increase in current with RF at frequencies up to 4 GHz and power levels above 10 dBm, and no effects at higher frequencies.

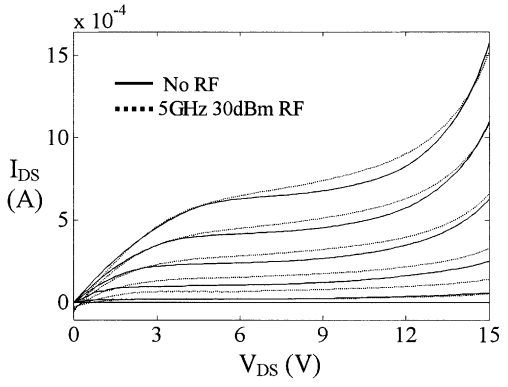

Fig. 3. Output current I_{DS} versus input bias V_{DS} with and without RF injection to the gate. Power effect is strongly suppressed by frequency: power 30 dBm, 5 GHz.

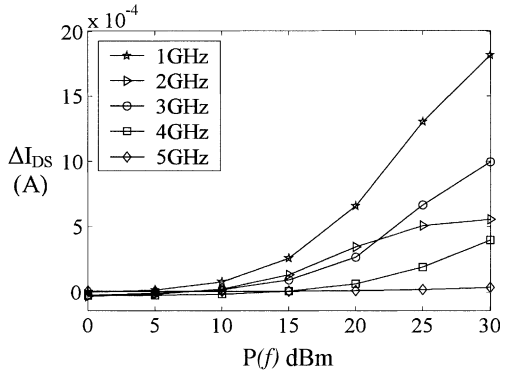

Fig. 4. Plot of drain current difference ΔI_{DS} with and without RF injection to the gate, versus injected power and frequency.

After the RF event the devices were measured again in order to identify permanent changes in their operational characteristics, but no discernible changes were observed. Hence these effects are categorized as "soft" error effects where the device may return to operation without permanent damage evident. RF Power injection to the drain electrode resulted in a decrease in drain current as shown in Fig. 5 (i.e. negative ΔI_D) for power levels up to 15 dBm, and then an increase (positive ΔI_D) at higher power levels, with the characteristics loosing saturation, and showing a significant reduction in breakdown voltage as shown in Fig. 6. A negative current offset at zero drain bias is evident, indicating the device starts operating at accumulation, before going into inversion at a drain bias around 0.5 V (Fig. 5). Again, at higher frequencies the power effect is strongly suppressed as in the case of gate injection. Fig. 7 shows the drain current plotted versus gate bias with and without RF injection at the gate. Under no RF injection the characteristics show good convergence and a

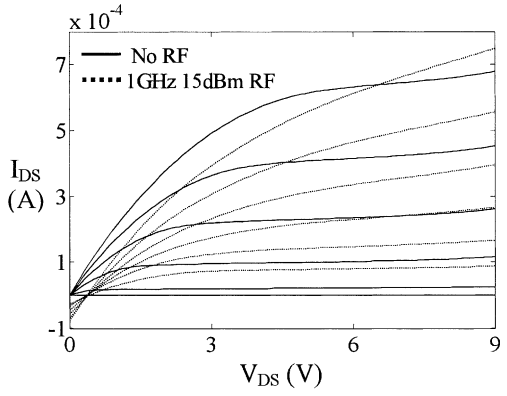

Fig. 5. Plot of drain current I_D versus input bias V_{DS} with and without RF injection to drain. Drain current decrease and negative offset current at zero drain bias are observed at power 15 dBm, 1 GHz.

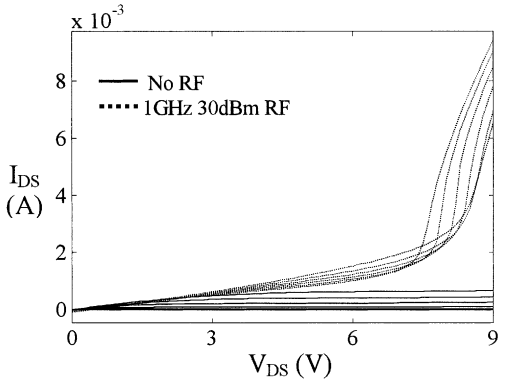

Fig. 6. Plot of drain current I_D versus input bias V_{DS} with and without RF injection to drain. Significant reduction in breakdown voltage and output current increase are observed at power 30 dBm, 1 GHz.

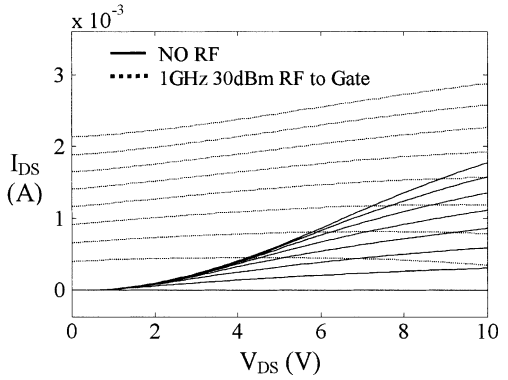

Fig. 7. Output current I_{DS} versus input bias V_{GS} with and without RF injection to the gate: no RF threshold voltage, $V_{th} = 1$ V. With RF on V_{th}, cannot be defined.

threshold voltage (V_{th}) of 1 V is measured. Under the RF injection however, lack of convergence of the characteristics is evident, indicating a fully-on channel with a high concentration of electrons where a threshold voltage cannot be defined. This demonstrates the inability of the channel to be effectively modulated by the gate bias which results in significant reduction in transconductance (g_m) as shown in Fig. 8. Significant decrease in g_m is observed at 1 GHz at 30 dBm for injection to the gate. However, at higher frequencies (5 GHz) the effect of power (30 dBm) is strongly suppressed and the transconductance value is restored. Injection to the drain gave similar results showing no convergence of the family of curves to define the threshold voltage, and a reduced transconductance for drain biases lower than 5 V. However, unlike the injection to the gate, an increase in transconductance is observed at drain biases close to the breakdown point (7 V), as shown in Fig. 9. Higher frequency (5 GHz) again strongly suppresses the effect of power as observed under gate injection also.

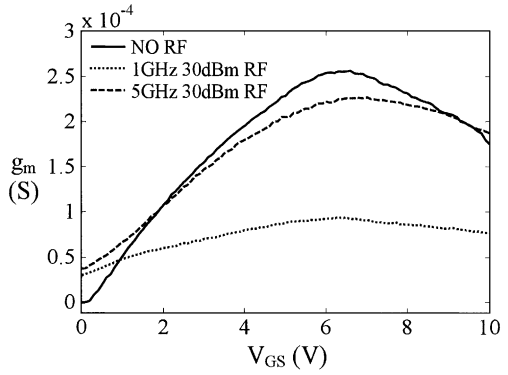

Fig. 8. Transconductance versus input bias V_{GS} with and without RF injection to the gate. Transconductance is observed to decrease significantly. At higher frequencies (5 GHz) power effects are suppressed and transconductance is restored.

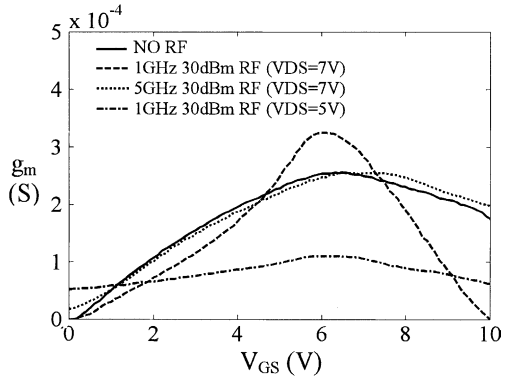

Fig. 9. Transconductance versus input bias V_{GS} with and without RF injection to the drain. Transconductance decreases significantly at drain bias $V_{DS} = 5$ V. At drain bias close to breakdown (7.0 V), transconductance increases. At higher frequencies (5 GHz) power effects are suppressed and transconductance is restored.

The sub-micron MOSFETs showed also the same trends in their operational parameters although the effects were not as pronounced due to lower power levels used to avoid burn-out and the difficulty to dissipate the injected power due to the by-pass capacitive effect at the gate and drain terminals. These devices were observed to be more vulnerable to the injection of RF power to the drain, due to gate oxide catastrophic failure at power levels above 18 dBm. *S*-parameter measurements of these devices are shown in Fig. 10 where the S_{11}, S_{12}, S_{21}, and S_{22} parameters are measured. Reflection parameters (S_{11}, S_{22}) of the injected RF power are observed to decrease with increasing frequency indicating that injected power must be dissipated (or transmitted) in the device. However, transmission parameters (S_{12}, S_{21}) remain constant and below one, indicating that the device has no gain and no significant power is transmitted. If we

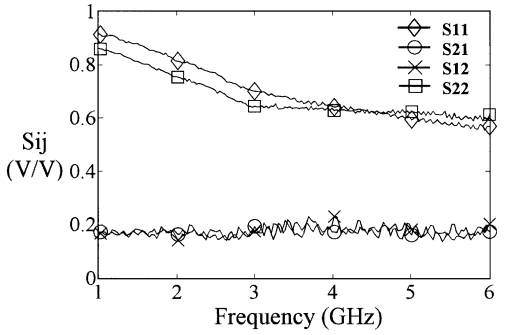

Fig. 10. Linear magnitude of *S*-parameters for sub-micron devices.

examine the small signal intrinsic capacitances of the devices, the capacitance values calculated for each mode of operation (saturation, triode, cut-off) show that the gate to ground capacitance and the drain to ground capacitances are the largest in value and therefore, as the frequency is increased these capacitors will be the first to become the by-pass capacitors providing a path for the RF injected signal to ground.

4. Conclusions

In conclusion, our study showed that injected microwave power at the gate and drain electrodes of n-channel MOSFET devices, significantly affects output current, transconductance, output conductance, and breakdown voltage for power levels above 10 dBm in the frequency range between 1 and 20 GHz. The effects result in loss of switching-off capability, loss of saturation and linearity in the amplification region, development of DC offset currents at zero drain bias, and substantial reduction in breakdown voltages. Most importantly the power effects were observed to be suppressed at frequencies above 5 GHz for these devices indicating the possibility of a by-pass path through intrinsic capacitive coupling to ground at the higher frequency range. Catastrophic failure "hard" errors were observed at power levels above 18 dBm for the sub-micron devices for RF injection to the drain due to gate oxide breakdown.

Acknowledgements

The support of AFOSR through the MURI Program is gratefully acknowledged. The help of J. Kim, G. Metze, J. Rodgers and T. Firestone is also gratefully acknowledged.

References

[1] M. Backstrom. HPM Testing of a Car. In Proceedings of the 13th International Zurich Symposium on EMC, Zurich, Switzerland, 1999.

[2] Chung DDL. Electromagnetic interference shielding effectiveness of carbon materials. Carbon 2001;39(2):279–85.
[3] Jana PB, Mallick AK, De SK. EMI shielding by carbon-fiber filled polychloroprene rubber composites. Composites 1991;22(6):451–5.
[4] Graffi S, Masetti G, Piovaccari A. Criteria to reduce failures induced from conveyed EMI on CMOS operational amplifiers. Microelectron Reliab 1997;37(1):95–113.
[5] Firestone TM, Rodgers JC, Granatstein VL. Measured RF induced non-linear effects in digital electronics. Proc ISDRS'03 2003:138–9.